JOURNAL OF CATALYSIS 79, 81–94 (1983)

Infrared Studies of CO Adsorption on Reduced and Oxidized Pt/TiO_2[1]

KATSUMI TANAKA AND J. M. WHITE[2]

Department of Chemistry, University of Texas, Austin, Texas 78712

Received April 18, 1982; revised August 17, 1982

Carbon monoxide adsorption experiments were studied on reduced and oxidized Pt/TiO_2 with FT-IR. On reduced samples two kinds of linear CO species were observed and assigned as adsorption on Pt close-packed (terrace) sites (2094 cm^{-1}) and on Pt open (step) sites (2077 cm^{-1}). In addition a bridged CO species was found at 1854 cm^{-1}. Both linear species show increasing frequencies with coverage. Saturation CO uptake decreases with increasing substrate reduction temperature and there is a preferential decrease of linear CO species on terrace sites and the concentration of bridged species lies below detection limits. On oxidized Pt/TiO_2 samples, some Pt atoms are covered with oxygen atoms and the density of step sites is enhanced. On these surfaces there are two kinds of linear CO species assigned to terraces (2130 cm^{-1}) and steps (2101 cm^{-1}) and a bridged CO species at 1880 cm^{-1}. In addition, several CO species are found which are also detected on reduced samples. These species show intensity variations during lengthy exposures. Preadsorbed linear CO species (2130, 2094, and 2077 cm^{-1} bands) on oxidized samples are also sensitive to H_2 exposures.

1. INTRODUCTION

The adsorption of CO is typically used in the characterization of supported metal catalysts. Since Eischens *et al.* reported adsorbed CO species on γ-Al_2O_3 and SiO_2 supported Pd, Ni, and Pt catalysts (*1*), much attention has been given to the type of CO, i.e., linear, bridged, and twin species (*2*). In general it is found that the CO adsorption depends on the metals themselves, their dispersion and oxidation state, as well as the support. Taking Pt catalysts for example, linear and bridged CO species are observed at 2040–2100 cm^{-1} and 1818–1865 cm^{-1} irrespective of their supported or nonsupported character; i.e., on Pt/γ-Al_2O_3 (*1, 3*), evaporated Pt film (*4*), Pt(111) (*5*), and Pt/Y-zeolite (*6*). An exception is the Pt/SiO_2 system where only a linear CO species is seen (*1*). Hopster and Ibach performed ELS and LEED measurements on Pt(111) and Pt 6(111) × (111) systems and observed linear CO species at 2089 cm^{-1} when the LEED pattern shows the $\sqrt{3} \times \sqrt{3}$ R30 structure while bridged species at 1885 cm^{-1} were involved in the C(4 × 2) structure (*7*).

It is reported that Pt supported on high-temperature prereduced TiO_2 shows a high catalytic activity for the photoassisted water decomposition and water gas shift reactions (*8*). TiO_2-supported metal catalysts also show striking CO and H_2 uptake decreases with increasing reduction temperature, called the strong metal support interaction (SMSI) (*9*), and high catalytic activity and selectivity are reported for such systems (*10*).

The aim of this paper is to characterize the CO adsorption sites both on oxidized and reduced Pt/TiO_2. Coadsorption experiments using $C^{16}O$ and $C^{18}O$ (1 : 1) and $C^{18}O$ exchange reaction with $C^{16}O$ preadsorbed species were performed on reduced catalysts as part of this characterization. In ad-

[1] Supported in part by the Office of Naval Research.

[2] Author to whom correspondence should be addressed.

0021-9517/83/010081-14$03.00/0

dition CO adsorption on oxidized Pt/TiO_2 and the subsequent effect of H_2 introduction was examined.

2. EXPERIMENTAL

A commercial anatase sample (MCB) was used as the support after overnight reduction with H_2 at 800°C. This is the same procedure used to obtain high activity for the photoassisted water decomposition reaction (*8*). The main impurities in the sample were As(0.0002%), Fe(0.010%), Pb(0.002%), and Zn(0.01%). Reduced TiO_2 was soaked in dilute chloroplatinic acid solution to prepare 2 wt% Pt loaded catalysts. This solution was dried at 100°C and the supported catalyst was washed with distilled water at 25°C until no chlorine was detected in solution. Carbon monoxide was purified through a 5A molecular sieve trap maintained at 77 K.

An infrared cell, with CaF_2 windows, was designed to prepare the sample *in situ* (*11*). Infrared spectra were recorded in absorbance using a Nicolet 7199 Fourier transform infrared spectrometer with 2 cm^{-1} resolution. Three hundred scans were taken to get good S/N. Absorption due to the windows and the gas phase were subtracted. CO was introduced to each sample at 25°C and infrared spectra were recorded at the same temperature.

Pellets for infrared experiments were prepared between pieces of paraffin paper mounted, using stopcock grease, to the faces of a 1-in.-diameter die. A pressure of 5000 lb $in.^{-2}$ was applied to 130 mg $in.^{-2}$ of powder. Without paraffin paper, attempts to prepare pellets were unsuccessful. There are advantages and disadvantages in this procedure. Metal contamination from the pellet die is minimized and sturdy infrared pellets are formed. However, pellets show paraffin adsorption bands which must be removed by oxidation at 400°C overnight. While we cannot rule out subtle changes in substrate structure as a result of this procedure no qualitative difference was observed for CO adsorption on Pt supported on unreduced anatase and the prereduced, reoxidized TiO_2 described above.

Carbon monoxide adsorption experiments were carried out on three kinds of samples: oxidized, reduced at 200°C, and reduced at 400°C. In each case the final step was evacuation at 400°C for 30 min. The three types are denoted as 400–NO–400, 400–200–400 and 400–400–400, where each number shows the treatment temperature in the following order: oxidation, reduction with H_2, and evacuation. Oxidation and reduction treatments were done in a static system. During reduction, 1 atm of purified hydrogen was replaced at least five times. The quantitative analysis of CO uptake gave CO/Pt = 0.20 on Pt/TiO_2 (400–200–400).

3. RESULTS AND DISCUSSION

In the sections below several CO stretching frequencies are assigned. These are summarized in Table 1, and the assignments of each band are summarized in Table 2.

3.1. CO Adsorption on Pt/TiO_2 (400–200–400)

CO absorption spectra on Pt/TiO_2 reduced at 200°C with H_2 overnight and subsequently evacuated at 400°C (400–200–400) are shown in Fig. 1. Introduction of 5 Torr CO, Fig. 1a, showed infrared absorption bands at 2185, 2092, and 1854 cm^{-1}. The 2092 and 1854 cm^{-1} bands can be assigned to linear and bridged CO on Pt, respectively, in agreement with the early work of Eischens *et al.* (*1*). The 2185 cm^{-1} band was observed in CO adsorption on TiO_2 and was assigned as a physisorbed species (*11*), however, the gas phase CO frequency is 2148 cm^{-1} so that it may be better to assign 2185 cm^{-1} as a weakly chemisorbed species. Upon evacuation at 25°C, Fig. 1a is converted to Fig. 1b; the 2185 cm^{-1} band disappears, the linear Pt–CO species shifts down to 2078 cm^{-1}, and the bridged CO remains at 1854 cm^{-1} but with lower intensity. This is quite dif-

TABLE 1

Experimental Conditions and Observed CO Band Frequencies

Experimental conditions	Observed frequency (cm^{-1})							
(1) 400–200–400 (Fig. 1)								
5 Torr CO ads. 25°C	2185	2094	—	1854				
Evacuation at 25°C	—	2078	—	1854				
Evacuation at 80°C	—	2074	2063	—				
Evacuation at 150°C	—	—	2060	—				
Evacuation at 200°C	—	—	—	—				
5 Torr CO ads. 25°C	2185	2094	2080	1854				
(2) 400–400–400 (Fig. 4)								
10 Torr CO ads. 25°C	2185	2083	—					
Evacuation at 25°C	—	2072	—					
Evacuation at 150, 200°C	—	—	2065	—				
6 Torr CO ads. 25°C	—	2075	—					
(3) 400–NO–400 (Fig. 5)								
0.8 Torr CO 25°C 5 min	2185	2097	—	1854	2130			
0.8 Torr CO 25°C 120 min	2185	2097	—	1854	2130	1880		
37 Torr CO 25°C 150 min	2185	2097	2077	1831	2120	1880		
37 Torr CO 25°C 63 hr	—	2094	2077	1854	2112	(1880)	2060	1942
Evacuation at 25°C	—	2094	2072	1854	—	—	—	(1942)
Evacuation at 150°C	—	—	2059	—	—	—	—	—
Evacuation at 200°C	—	—	—	—	—	—	—	—
5 Torr CO 25°C 5 min	2185	2096	2080	1854	2131	—	—	—
(4) O_2 400–NO–400 (Fig. 7)								
7 Torr CO 25°C 7, 80 min	2185	2098	—	1854	2130	—		
Evacuation at 25°C	—	2092	2080	1854	2128	—		
Evacuation at 100°C	—	—	2055	—	2131	—	2101	

ferent from the behavior on alumina-supported Pt catalysts, where the bridged species is easily removed during evacuation at 25°C (*3a*). Spectrum 1c, after evacuation at 80°C, showed no bridged species and an adsorption maximum at 2063 cm^{-1} with a shoulder at 2074 cm^{-1}. After 150°C evacuation this shoulder disappeared leaving a single peak at 2060 cm^{-1} (Fig. 1d). No CO remained after evacuation at 200°C (Fig. 1e). In order to check the reproducibility, 5 Torr CO was introduced after experiment 1e. As shown, Fig. 1f reproduces Fig. 1a except the shoulder at 2082 cm^{-1} is resolved and there is a 20% decrease in intensity.

TABLE 2

Assignment of CO Bands

Frequency/cm^{-1}	Species	Site
2185	L[a]	TiO_2
2130	L	$Pt(O_a)$/terrace
2101	L	$Pt(O_a)$/step
2094	L	Pt/terrace
2077	L	Pt/step
1880	B	Pairs of $Pt(O_a)$
1854	B	Pairs of Pt
2060, 1942	T	Edge Pt

[a] L, B, and T denote linear, bridge, and twin sites. $Pt(O_a)$ denotes oxygen covered Pt.

The downward frequency shift of linear CO frequency with decreasing CO coverage is a common observation. One of the earliest observations was for CO on Pt/SiO_2 where the shift was from 2067 to 2040 cm^{-1}, a shift attributed to dipole–dipole interactions (*12*). However, Blyholder (*13*) proposed that the formation of a strong bond enhances back donation from metal *d*-orbitals to antibonding $2\pi^*$ orbital of the CO

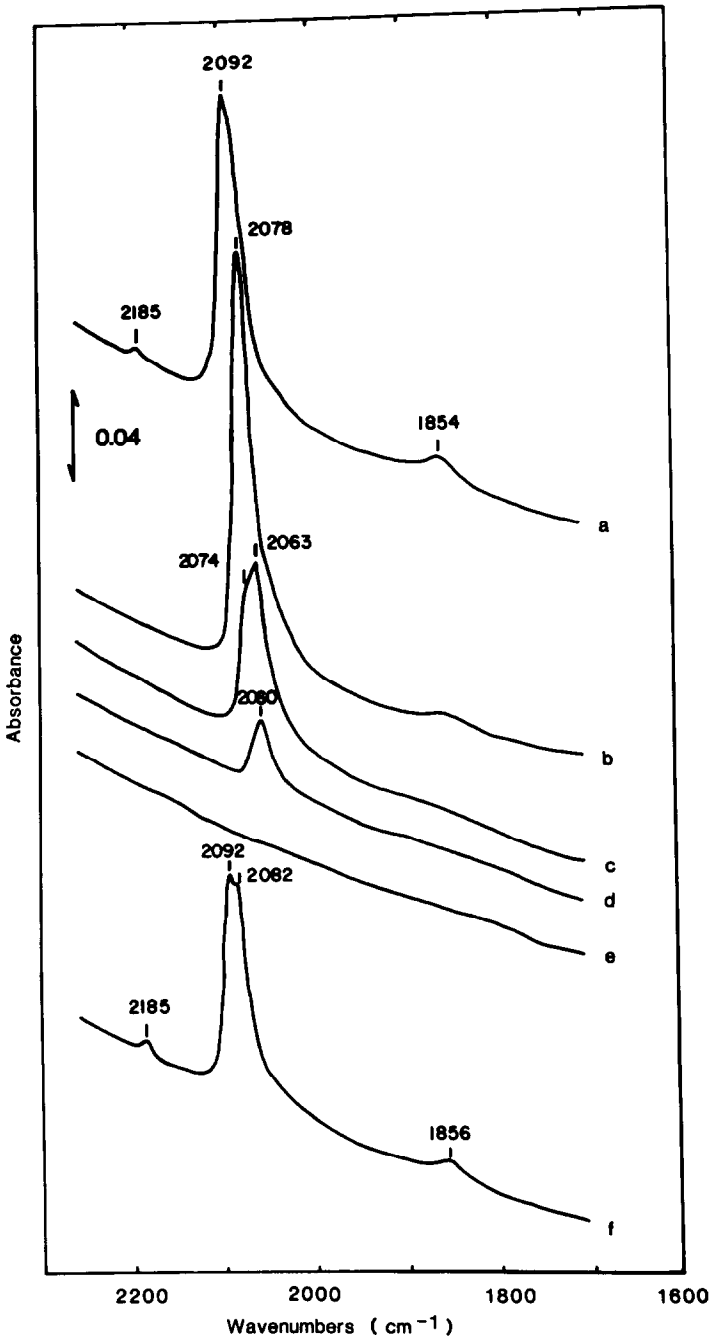

FIG. 1. Spectra for CO adsorption on Pt/TiO_2 reduced at 200°C (400–200–400). (a) 5 Torr CO. (b) Evacuation of (a) at 25°C. (c) Evacuation at 80°C. (d) Evacuation at 150°C. (e) Evacuation at 200°C. (f) 5 Torr of CO after (e).

molecule, thereby weakening the C–O bond. This would cause the frequency to shift downward. Since the metal–CO bond energy typically decreases with coverage, we would expect the stretching frequency to decrease as the coverage decreases. As Hollins and Pritchard (*14*) suggest, this kind of explanation is chemical in nature

and has a quite different origin than the dipole–dipole interactions.

Reflection–absorption infrared spectra for CO on polycrystalline Pt, dominated by the (111) face, show a frequency shift from 2065 to 2101 cm^{-1} as the coverage increases to saturation (*5a*). Crossley and King (*5b*) use a model, first developed by Hammaker *et al.* (*12*), to account for this frequency shift. It involves experimental vibrational spectra, from isotopic mixtures of ^{13}CO and ^{12}CO. If the shift of the ^{12}CO band to higher frequency with increasing coverage is due only to dipole–dipole interactions, then successive substitution of ^{12}CO with ^{13}CO, at constant total coverage so the metal–CO interaction is constant, should reduce the frequency. They obtained this result experimentally. The essential feature of the model is the frequency shift, which is proportional to the lattice sum, ΣR_{ij}^{-3}, where R_{ij} is the distance between the centers of two dipoles i and j. Similar coverage induced frequency shifts have been reported for linear CO on evaporated Ir (*15*), Ir/SiO_2 prepared from $Ir_4(CO)_{12}$ (*16*), and γ-alumina supported Pt (*3b*). Frequency shifts are also detected for bridged CO on Ni (*17*) and Pd (*18*).

To test whether or not the shift shown in Fig. 1 was due to dipole–dipole interactions, equimolar $C^{16}O$ and $C^{18}O$ (6 Torr) was introduced on Pt/TiO_2 (400–200–400). As shown in Fig. 2a, linear $C^{16}O$ and $C^{18}O$ species on Pt were observed at 2074 and at 2007 cm^{-1}. On TiO_2, $C^{16}O$ and $C^{18}O$ gave bands at 2185 and 2135 cm^{-1}. Isotopically different bridged species were not resolved here; however, bridged $C^{16}O$ and $C^{18}O$ species were resolved at 1854 and 1810 cm^{-1} using a different procedure (Fig. 3). After evacuation at 25°C, the 2074 cm^{-1} band shifted to 2061 cm^{-1}, while the relative intensity of the shoulder at 2007 cm^{-1} grew with no frequency shift. These two bands shifted to lower frequency with lower CO coverage as the evacuation temperature was increased to 80°C (Fig. 2c and to 150°C (Fig. 2d). Evacuation at 200°C (Fig. 2e) left

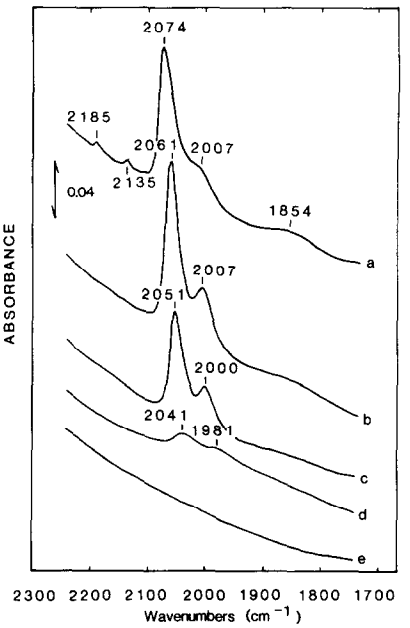

FIG. 2. Adsorption of an equimolar mixture of $C^{16}O$ and $C^{18}O$ on Pt/TiO_2 (400–200–400). (a) 6 Torr of mixture. (b)–(e) Evacuation of (a) at 25, 80, 150, and 200°C, respectively.

no detectable adsorbed CO. Comparing 1a with 2a and 1b with 2b, we note that under similar coverage conditions the $C^{16}O$ stretching frequency is always reduced in the presence of $C^{18}O$.

Eischens *et al.* (*1*) observed two bands at 2074 and 2012 cm^{-1} when a mixture of ^{12}CO and ^{13}CO was adsorbed on a Pt/SiO_2 catalyst. (Note that the isotope effect of $^{13}CO/^{12}CO$ is almost the same as $C^{18}O/C^{16}O$ so results can be compared directly.) They find that chemisorbed CO is pumped out at 200°C and that the relative intensities of the two bands depends on the surface coverage with the high-frequency band becoming relatively more intense as the surface coverage increases, just as we observe in Fig. 2. This is interpreted in terms of dipole coupling variations.

Our results are quite consistent with theirs. We conclude that for CO on Pt/TiO_2 (400–200–400) the 2092 cm^{-1} band is a linear species and the frequency shift of this species can be interpreted completely in

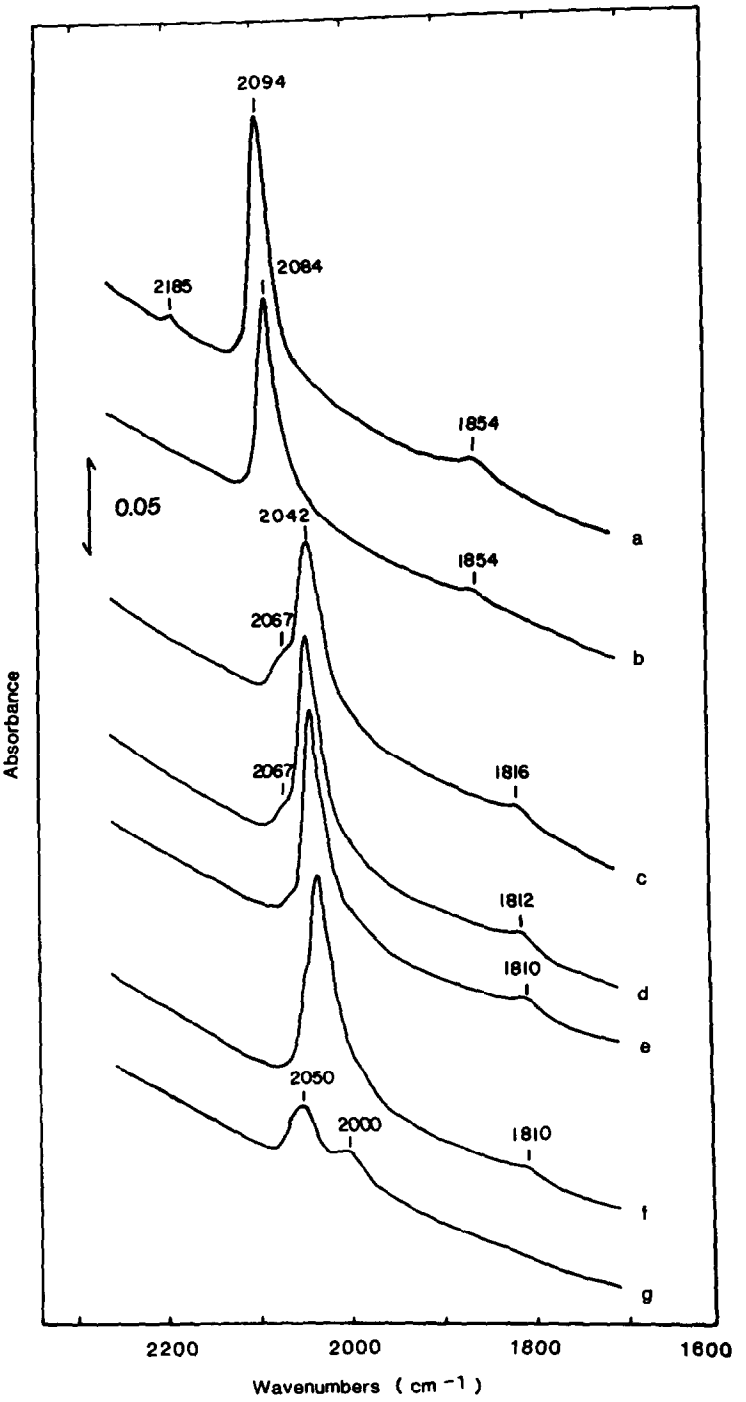

FIG. 3. Exchange of $C^{18}O$ with presorbed $C^{16}O$ on Pt/TiO_2 (400–200–400). (a) 8 Torr $C^{16}O$. (b) Evacuation of (a) at 25°C. (c)–(e) Exposure of (b) to 3 Torr $C^{18}O$ for 5 min, 30 min, and 18 hr, respectively. (f)–(g) Evacuation of (e) at 25 and 80°C, respectively.

terms of dipole–dipole interactions between absorbed species.

The exchange of $C^{18}O$ with $C^{16}O$ preadsorbed on Pt/TiO_2 at 25°C was used as a

complement to the adsorption experiment described above. First 8 Torr of $C^{16}O$ was dosed onto a 400–200–400 Pt/TiO_2 sample (Fig. 3a), and followed by evacuation at 25°C (Fig. 3b). When this surface was exposed to 3 Torr $C^{18}O$, the linear $C^{16}O$ species on Pt changed to the $C^{18}O$ homolog at 2042 cm^{-1}, with a shoulder at 2067 cm^{-1}, and bridged $C^{16}O$ at 1854 cm^{-1} changed quickly (5 min) to bridged $C^{18}O$ at 1816 cm^{-1} (Fig. 3c). The shoulder at 2067 cm^{-1} gradually decreased in intensity with time of exposure to $C^{18}O$; Fig. 3d is after 30 min and Fig. 3e is after 18 hr. During this same period the bridged CO species moved to 1810 cm^{-1}. The isotope frequency ratios of the 1810/1854 cm^{-1} and 2042/2094 cm^{-1} bands are consistent with the theoretical value (0.9759).

Evacuation at 25°C (Fig. 3f) had little effect on the spectrum but, upon evacuation at 80°C, two bands were observed at 2050 and 2000 cm^{-1} (Fig. 3g). It is very interesting to compare this with Fig. 2c which was recorded after evacuation at the same temperature following a 1 : 1, $C^{16}O : C^{18}O$; adsorption experiment. About 90% of all the adsorbed $C^{16}O$ on Pt exchanges readily with $C^{18}O$. The remaining 10% is associated with the $C^{16}O$ species at 2067 cm^{-1} (Fig. 3e), and does not exchange readily. This $C^{16}O$ species is adsorbed strongly and remains, with a frequency shift to 2050 cm^{-1}, after evacuation at 80°C (Fig. 3g). The equilibration of isotopic species in the exchange is heavily weighted in favor of adsorbed $C^{18}O$ because of the dominance (50/1) of $C^{18}O$ in the gas phase. These results imply that adsorbed $C^{16}O$ species which rapidly exchange with gas phase $C^{18}O$ at 25°C are those species removed by evacuation at 80°C. Moreover, the evidence suggests that the CO species at 2060 cm^{-1} remaining after evacuation at 150°C (Fig. 1d) and after the exchange reaction with $C^{18}O$ (Figs. 3c,g), is not the same species as that showing a strong band at 2094 cm^{-1} (Figs. 1a, and 3a). We propose that the 2094 cm^{-1} band is due to CO on terrace sites while the band at 2050 cm^{-1} involves step site adsorption. In the following paragraphs we relate this idea to observations on unsupported metals.

According to X-ray diffraction results for the Pt/TiO_2 system, the surface of supported Pt is composed mainly of (111) faces with a small amount of the (200) face (*9a, 19*). It is also well known that the (111) face is dominant for annealed polycrystalline Pt (*20*). Therefore it is worthwhile considering CO adsorption experiments done on Pt(111). Several studies (*21–23*) of CO adsorption on Pt(111) indicate that the activation energy for desorption drops monotonically with CO coverage and that the activation energy for desorption, extrapolated to zero coverage, is about 33 kcal $mole^{-1}$. In these experiments there is no evidence for the different kinds of species and sites that would account for the distinctly different isotope exchange rates that we observe.

Stepped or kinked Pt(111) does show site heterogeneity in CO desorption; two peaks appear (*7, 24–26*), and the intensity ratio follows the step/terrace concentration ratio. While there are significant variations in the quoted activation energies for desorption, there is agreement that desorption from step sites involves at least 3 kcal $mole^{-1}$ higher activation energy than desorption from the terrace sites. Consequently, it is not unreasonable to expect some variations in isotopic molecular exchange rates. If CO adsorbed at step (and other defect) sites exchanges slowly, compared to CO adsorbed at terrace sites, then we would expect this to be reflected in experiments like those summarized in Fig. 3. Thus we interpret the 2050 cm^{-1} band in Fig. 3g as $C^{16}O$ adsorbed on step sites. Note the similarity between Fig. 2d and Fig. 3g.

Because connections to single crystal work involving the step/terrace concepts are made here we have chosen to use this language. It should be recognized that one could also use the language of closed-packed (111) and open (higher index) crystallite faces.

Recently Bartok *et al.* (*27*) found adsorp-

tion–desorption hysteresis curves in CO on Pt supported Cab-o-sil systems, where high-frequency "adsorptive CO" is ascribed to disordered species while low-frequency "desorptive CO" is ascribed to ordered species. According to their results, CO molecules migrate from low Miller index planes, terraces, to high Miller planes, steps and kinks, prior to desorption. Their observations with respect to surface heterogeneity are consistent with our results.

3.2. CO Adsorption on Pt/TiO_2 (400–400–400)

Adsorption of CO was carried out on Pt/TiO_2 after overnight oxidation followed by reduction and evacuation, all at 400°C (Fig. 4). We selected 400°C as the maximum hydrogen reduction temperature (which gives a mild SMSI system) because a complete SMSI system (reduced at 500°C) is known to reduce the CO uptake at 25°C by as much as a factor of 20 (*9, 19*). Under these conditions, CO bands are difficult to detect. In an ambient of 10 Torr CO (Fig. 4a), infrared absorption was recorded at 2185 and 2083 cm^{-1} which correspond to CO on TiO_2 and linear CO on Pt, respectively. It is noteworthy that the intensity of the CO species on Pt decreased by about 50% relative to the spectrum of Fig. 1a. Moreover, no bridged CO species was seen. This is not merely a signal-to-noise problem since a 50% reduction of the 1854 cm^{-1} band of Fig. 1a would still be easily measured. As shown in Fig. 4b, the linear CO species on Pt at 2083 cm^{-1} shifted to 2072 cm^{-1} upon evacuation at 25°C for 30 min. Following this procedure, 1 atm CO was added (Fig. 4c). Approximately the same intensity CO band as observed in Fig. 4a was seen at 2081 cm^{-1} with some complicated bands at around 2170 cm^{-1}. Evacuation at 25 and 150°C (Figs. 4d,e) caused a frequency shift of linear CO species on Pt from 2081 to 2075 cm^{-1} and 2065 cm^{-1} with accompanying losses of intensity. In Fig. 4d two small intensity bands were detected around 1940 and 1840 cm^{-1}. These are not associated with CO since they often appear on reduced samples in the absence of CO. Although the origin of these bands is unknown, they may be associated with overtones of Ti–O lattice vibrations. The 2065 cm^{-1} band remained following evacuation at 200°C (Fig. 4f). This is quite different from the behavior shown by Pt/TiO_2 reduced at only 200°C (Figs. 1–3) where all the CO bands disappear after evacuation at 200°C.

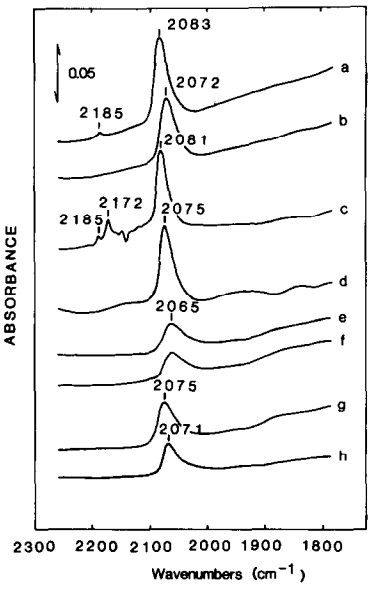

FIG. 4. CO adsorption on Pt/TiO_2 (400–400–400). (a) 10 Torr CO. (b) Evacuation of (a) at 25°C. (c) 1 atm CO after (b). (d)–(f) Evacuation of (c) at 25, 150, and 200°C, respectively. (g) 6 Torr CO after (f). (h) Evacuation of (g) at 25°C.

After the spectrum of Fig. 4f was taken, the sample was exposed to 6 Torr of CO in order to check reproducibility. As indicated in Fig. 4g, the frequency of CO on Pt shifted to 2075 cm^{-1} as compared to 2083 cm^{-1} in Fig. 4a. Moreover, the intensity decreased about 50%. Evacuation at 25°C led to the expected downward frequency shift (Fig. 4h). Taking difference spectra (not shown), i.e., 4b − 4a and 4h − 4g, clearly indicates that those species giving the 2080 cm^{-1} band partially rearranged and partially desorbed with evacuation to give the bands in the 2065–2071 cm^{-1} range. This suggests that either: (i) a CO molecule on a terrace

migrates and is stabilized on a step or defect site or (ii) that CO molecules adsorb primarily on step sites and, upon evacuation, the frequency of this band moves down due to lower dipole–dipole interactions. We favor the former explanation.

The uptake of both H_2 and CO on TiO_2-supported noble metal catalysts is strongly diminished by H_2 reduction at 500°C. This is not the result of metal agglomeration on the TiO_2 support since more than $\frac{2}{3}$ of the original CO and H_2 uptake is recovered by reoxidation at 600°C (*8*). This characteristic is called the strong metal–support interaction (SMSI) and has been shown to give significant effects in CO hydrogenation activity and selectivity (*10*).

The morphology of the Pt particles is significant. Baker *et al.* (*28*) conclude from transmission electron microscopy that Pt on TiO_2 (in the SMSI state) is in the form of thin hexagonal pillboxes grown over a partially reduced titania, Ti_4O_7. The faces of these thin structures have Pt(111) character with mainly terrace sites. It is this structure which shows only weak CO chemisorption. Our results then suggest that a selective decrease in CO binding on terrace sites, perhaps due to changes in the Pt electronic structure, leads to the loss of CO chemisorption activity.

From LEED and high-resolution electron energy loss spectroscopy (HREELS) data, there are two ordered structures showing different CO binding on Pt(111) (*7*). For the $\sqrt{3} \times \sqrt{3}$ R30° structure, only linear bonding is found while for the c(4 × 2) structure, both the linear (2089 cm^{-1}) and bridged (1855 cm^{-1}) structures are found. On a stepped surface, 6(111) × (111), a linear species at 2089 cm^{-1} is also found even when the thermal desorption spectra clearly indicate that CO is bound only to step sites. The relatively low resolution of HREELS (≈60 cm^{-1}) may have prevented observation of shifts due to binding differences on terraces and steps (*29*). These results are not inconsistent with the notion that, in the SMSI system, terrace sites become dominant, that no bridge bonded CO

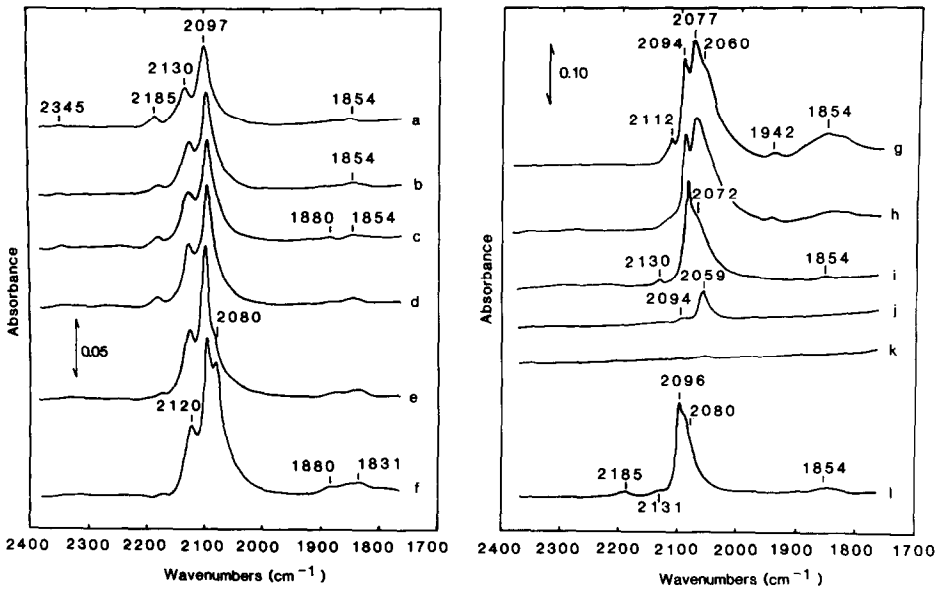

FIG. 5. CO adsorption spectra on oxidized Pt/TiO_2 (400–NO–400). CO pressure was increased from 0.8 to 37 Torr after 120 min. Exposure times were: (a) 5 min, (b) 60 min, (c) 120 min, (d) 125 min, (e) 180 min, (f) 270 min, and (g) 65 hr. After (g) the system was evacuated at: (h) 25°C, (i) 80°C, (j) 150°C, and (k) 200°C. (l) 5 Torr CO after (k).

is present on step sites, and that linear CO binding on residual steps is still strong.

3.3. *CO Adsorption on Pt/TiO_2 (400–NO–400)*

Adsorption of CO on Pt/TiO_2 that was oxidized at 400°C and evacuated at 400°C (400–NO–400) proved very interesting because various absorption bands changed position and intensity during the time of the experiment. Figure 5a shows that when an oxidized Pt/TiO_2 was exposed to 0.8 Torr CO at 25°C, bands were observed at 2345 (CO_2 on TiO_2), 2185 (CO on TiO_2), 2130 and 2094 (linear CO on Pt), and 1854 cm^{-1} (bridged CO on Pt). With exposure time (Figs. 5b and c) the intensity of the 2130, 2094, and 1854 cm^{-1} bands gradually increased. The formation of a small new band was detected at 1880 cm^{-1} after 120 min (Fig. 5c). In the early stages of this experiment, bidentate carbonate and bicarbonate species on TiO_2 were observed at 1590 and 1430 cm^{-1}.

After a 120-min exposure to 0.8 Torr CO, the CO pressure was raised quickly to 37 Torr. The spectrum after 5 min (Fig. 5d) indicates that the intensity of the 2185 cm^{-1} band decreased slightly while the 2345 cm^{-1} band (coordinated CO_2 on TiO_2) disappeared and bidentate carbonate and bicarbonate were detected in smaller amounts than under the conditions of Fig. 5c. With time, 180 min in Fig. 5e, a shoulder appeared at 2080 cm^{-1} and grew to dominate the spectrum after 65 hr (Fig. 5g). During the same period, the 2185 cm^{-1} band disappeared, a relatively intense shoulder appeared at 2060 cm^{-1}, the 2130 cm^{-1} band shifted downward to 2112 cm^{-1}, a band appeared at 1942 cm^{-1}, and the intensity in the 1854 cm^{-1} region increased significantly. Note that the sensitivity in Figs. 5a–f is twice that of the other spectra in Fig. 5.

Figure 6 shows the time dependence of the intensities of three of these bands. It is noteworthy that the 2080 cm^{-1} band is sensitive to the CO pressure and the 2130 cm^{-1} band goes through a maximum and then

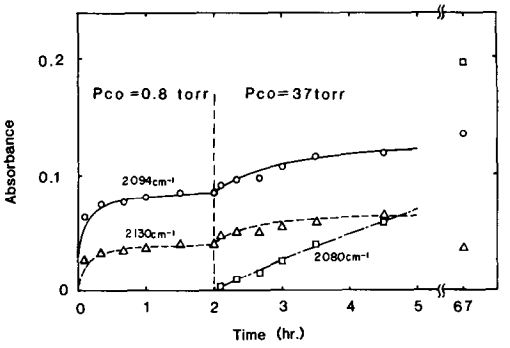

FIG. 6. Time dependence of intensity changes for spectra of Fig. 5.

decreases (compare 4.5 and 67 hr in Fig. 6). Other experiments show that the formation rate of the 2080 cm^{-1} band depends both on the CO pressure and the relative amount of the 2130 cm^{-1} band. The spectral changes shown in Figs. 5 and 6 were reproducible after a reduction–oxidation cycle of the Pt/TiO_2.

Spectra h through k of Fig. 5 characterize the thermal stability of the CO/Pt/TiO_2 system of Fig. 5g after evacuation at temperatures between 25 and 200°C. Upon evacuation at 25°C (Fig. 5h) the intensity of the 2112, 2060, 1942, and 1854 cm^{-1} bands all decreased. Spectrum i, obtained after evacuation at 80°C, shows selective desorption of the 2077 cm^{-1} band and further losses at 1942 and 1854 cm^{-1}. In the region above 2100 cm^{-1}, there was significant loss of intensity associated with a 2101 cm^{-1} band (see below) which allowed a small band at 2130 cm^{-1} to be observed clearly. Evacuation at 150°C (Fig. 5j) was accompanied by a 20-fold loss of 2094 cm^{-1} intensity and by a shift of the 2077 cm^{-1} band to 2059 cm^{-1} with a 70% loss of intensity. Evacuation at 200°C completely removed the adsorbed CO species (Fig. 5k).

After evacuation at 200°C, the sample was re-exposed to 5 Torr CO. Figure 5l, taken after 5-min exposure to 5 Torr CO, shows that the 2130 cm^{-1} band is a factor of 10 weaker relative to spectrum 5a and that the formation of the 2080 cm^{-1} species was much faster than shown in Figs. 5a–g. This

result is interpreted to mean that the surface of oxidized Pt/TiO_2 is reduced with CO and the formation rate of the 2080 cm^{-1} intensity is inversely proportional to the intensity of the 2130 cm^{-1} band.

The results of a series of experiments, like those of Fig. 5, can be summarized as follows (see Table 1 for assignments):

(a) On a Pt/TiO_2 surface predosed with O_2 at 400°C exposure to CO leads to bands associated with and without interacting oxygen. The former is found at 2130 cm^{-1} (Fig. 5a) and the latter at 2097 and 2077 cm^{-1} (Fig. 5g). The formation rate of the 2077 cm^{-1} band is dependent on the CO pressure.

(b) On the same surface there are two kinds of bridged CO (1880 and 1854 cm^{-1}). The intensities of the 1880 and 2130 cm^{-1} bands are related. These are assigned (see below) to CO adsorbed in bridged and linear forms that also involve chemisorbed oxygen.

(c) With exposure time, the 2130 cm^{-1} band reaches a maximum intensity and shifts to lower frequency. This species is ascribed to linear CO on Pt with interacting oxygen since the intensity decreased sharply following surface reduction.

(d) The intensity decrease with time of the physisorbed CO species on TiO_2 at 2185 cm^{-1} is associated with the formation of coordinated CO_2 at 2345 cm^{-1}, as well as some carbonate species, on TiO_2.

In the previous sections we suggested two kinds of CO on Pt/TiO_2, terrace and step Pt(111) sites. This also appears to be the case for oxygen predosed Pt/TiO_2. Before considering the details, we briefly consider the interaction of O_2 with Pt. Molecularly adsorbed, atomically chemisorbed, and subsurface oxide are all known to exist in the O_2/Pt(111) system (*30*). In our system molecular adsorption is negligible since the sample is evacuated at 400°C. We expect the oxygen to be predominately chemisorbed atomic species although, for small Pt particles on TiO_2, subsurface oxygen may be formed. This remains an open question deserving further study. We attribute the 2130 cm^{-1} band to CO on Pt in the presence of atomic oxygen.

On well-characterized bulk single crystals, dissociation of O_2 on Pt takes place mainly on step sites, as compared to terrace sites (*25*). Assuming, then, that oxygen atoms are chemisorbed primarily on step sites in our system, we expect selective CO adsorption on terrace sites (2094 cm^{-1}) until the oxygen atoms at the steps are removed. The CO pressure dependence of the 2080 cm^{-1} band (Fig. 6), which is assigned to CO on step sites, can be interpreted in terms of selective adsorption of oxygen atoms on these sites followed by a slow reaction with CO, removal as CO_2, and, finally, CO adsorption at the same sites.

In a supporting experiment, a (400–NO–400) sample was exposed to 1 atm of O_2 for 30 min at 25°C, evacuated at 25°C, and exposed to 7 Torr of CO at 25°C. Comparing Figs. 7a and b with Figs. 5a and b, there are no qualitative differences suggesting that the adsorbed oxygen reactivity and structure do not depend on either the

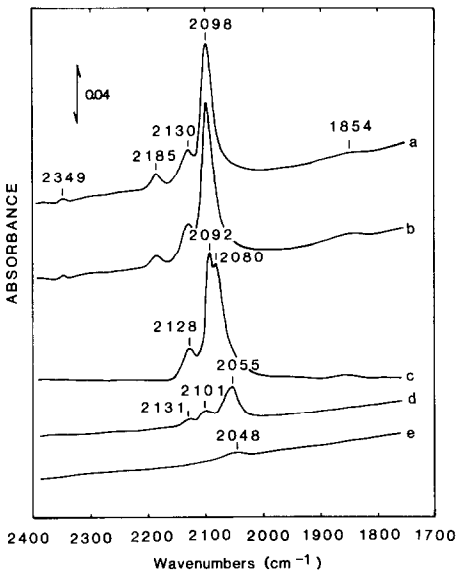

FIG. 7. CO adsorption on an oxidized Pt/TiO_2 (400–NO–400) redosed with O_2 at 25°C. Exposure of 7 Torr CO for (a) 7 min and (b) 80 min. Evacuation of (b) at: (c) 25°C, (d) 100°C, and (e) 200°C.

adsorption or evacuation temperature between 25 and 400°C. Figure 7c shows that the 2080 cm^{-1} band intensity grew in during evacuation at 25°C. We take this to mean that step sites were vacated during evacuation by reaction of CO with O(a) and removal as CO_2, thereby allowing terrace CO to migrate to the step sites. Spectrum 7d, seen after evacuation at 100°C, shows that the 2130 cm^{-1} band is composed of two species with frequencies at 2130 and 2101 cm^{-1}.

The presence of two kinds of CO on oxygen covered Pt reminds us that there are two kinds of CO on reduced Pt, terrace and step species. If it is assumed that the 2130 and 2101 cm^{-1} bands correspond to terrace and step adsorption on oxygen-covered Pt, then the downward frequency shift of mixtures of these two species in Fig. 5 can be accounted for as the result of enrichment of the 2101 cm^{-1} band. This assignment is supported by another experimental result. In Fig. 6 there is a linear relationship between the absorbance of the 2094 and 2130 cm^{-1} bands during the first 2 hr of the exposure, where the frequency of the CO on oxygen covered Pt remains at 2130 cm^{-1}.

The remaining assignments involve the bands at 2060 and 1942 cm^{-1}. These may be assigned to dicarbonyl species. If present, such species should give a pair of bands (symmetric and asymmetric) as in $Ir(CO)_2$ (*16*) and $Rh(CO)_2$ (*31*). These species formed on λ-alumina are thought to be on partially oxidized isolated metal sites like Rh^I. The formation of such species would require extensive coordinative unsaturation as expected at steps, kinks, and other defects, McClellan *et al.* (*26*) suggest that for the Pt(321) surface made of rough steps which have a high density of kinks, 40% of the surface Pt atoms are coordinatively unsaturated. Such surface sites could account for the formation of dicarbonyl species.

The results of introducing H_2 to a Pt/TiO_2 surface, predosed with CO and evacuated at 25°C, are shown in Fig. 8. Prior to the introduction of H_2, the intensities of the

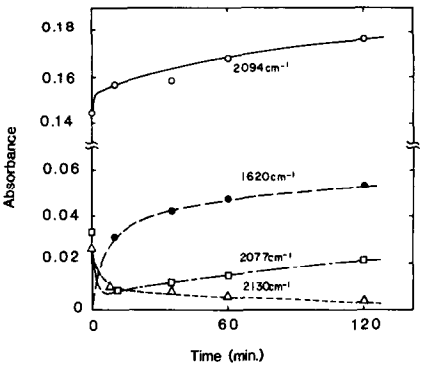

FIG. 8. Effect of H_2 (1 atm) introduction on a Pt/TiO_2 sample predosed with CO.

2094, 2077, and 2130 cm^{-1} bands were 0.144, 0.033, and 0.028, resepctively. Adding H_2 gave rise to a rapid intensity increase in the 2094 cm^{-1} band and an abrupt decrease of the 2077 and 2130 cm^{-1} bands. With H_2 exposure time, Fig. 8 shows that the 2094 and 2077 cm^{-1} band intensities increase gradually, while the band at 2130 cm^{-1} decreased slowly. After a 2-hr exposure, the frequencies of these three bands shifted down to 2080, 2062, and 2118 cm^{-1}. The combined intensity of the 2094 and 2077 cm^{-1} bands was 0.178 at the start and rose to 0.196 after 2 hr. This increase matches nicely the intensity lost (0.019) in the 2130 cm^{-1} band and indicates that CO molecules on oxygen covered Pt are converted to CO species on step and terrace sites on reduced Pt during H_2 exposure. The growth of the 1620 cm^{-1} band, indicating water formation, is consistent with the above frequency shifts in the sense that surface reduction is occuring. Cavanagh and Yates (*32*) as well as Apple and Dybowski (*33*) studied the effect of coadsorption of CO on the adsorption of H_2 on Rh/Al_2O_3 and Rh/TiO_2 and concluded that preadsorbed CO inhibits the adsorption of "spillover" hydrogen. Applied to our system, we expect no reduction of TiO_2 and interpret the water indicated in Fig. 8 as arising from reaction with oxygen on Pt (hydrogen titration).

Two of the more interesting results of the experiment described in Fig. 8 are the

downward frequency shift with time of the CO species on both step and terrace sites and the abrupt intensity changes in some of the bands just after hydrogen introduction. Downward frequency shifts are also observed in coadsorption of H_2O and CO. This is explained in terms of strengthened chemical bonds between Pt and C. Though there is no hydrogen adsorption data that compare the characteristics of terrace and step sites, our intensity redistribution data suggest that: (a) most CO molecules on Pt are mobile and (b) hydrogen adsorbs in a way that removes some CO from step sites. Since H_2 adsorption is not likely to induce CO desorption, we expect that CO molecules removed from step sites will migrate to terrace sites. This result implies that CO and H on step sites have different adsorption structures than their counterparts on terrace sites. The initial sticking coefficient for H_2 is reported to be 0.2 for clean Pt(111) and 0.4 for oxygen covered Pt(111); however, the saturation coverage for H(a) is nearly the same in both cases (*23*). Taking this result over to our supported Pt system, hydrogen adsorption would occur more readily on step sites since oxygen atoms prefer to adsorb there.

4. SUMMARY

The ir data reported here show clearly that a variety of adsorbed CO species are observed on platinized titania depending on the pretreatment of the adsorbate. The absorption bands are interpreted in terms of the traditional bridged and linear CO species. Here, we find two types of linear CO species which are assigned to adsorption on terrace (close-packed) and step (open) sites. Detectable frequency shifts in both are found in the presence of interacting oxygen. Exchange experiments involving $C^{18}O$ and $C^{16}O$ demonstrate that the species attributed to step sites exchange more slowly than those at the terrace sites. This is confirmed by thermal desorption experiments showing that the higher frequency linear CO component (terrace site) is less stable. In the strongly reduced SMSI state, Pt/TiO_2 adsorbs small amounts of CO, bridged CO is not detected, and adsorption at terrace sites is lost preferentially. On oxidized Pt/TiO_2, several kinds of adsorbed CO form and intensities are time dependent reflecting oxygen removal by reaction with CO to form CO_2, particularly at step sites. Under some conditions, weak bands assigned to dicarbonyl are found. Finally, exposure of a CO-predosed sample to H_2 causes marked changes in the intensities of certain CO bands indicating surface reduction to form water and a redistribution of linearly bound CO between step and terrace sites.

REFERENCES

1. (*a*) Eischens, R. P., Francis, S. A., and Pliskin, W. A., *J. Phys. Chem.* **60,** 194 (1956). (*b*) Eischens, R. P., and Pliskin, W. A., *Adv. Cataly.* **10,** 1 (1958).
2. Ugo, R., *Catal. Rev.* **11,** 255 (1975).
3. (*a*) Peri, J. B., *J. Catal.* **52,** 144 (1978). (*b*) Rothchild, W. G., and Yao, H. C., *J. Chem. Phys.* **74,** 4186 (1981).
4. (*a*) Garland, C. W., Lord, R. C., and Troiano, P. F., *J. Phys. Chem.* **69,** 1188 (1965). (*b*) Blyholder, G., and Sheets, R., *J. Phys. Chem.* **74,** 4335 (1980).
5. (*a*) Shigeishi, R. A., and King, D. A., *Surface Sci.* **58,** 379 (1976). (*b*) Crossley, A., and King, D. A., *Surface Sci.* **68,** 528 (1977).
6. Primet, M., Fouilloux, P., and Imelik, B., *J. Catal.* **61,** 553 (1980).
7. Hopster, H., and Ibach, H., *Surface Sci.* **77,** 109 (1978).
8. (*a*) Sato, S., and White, J. M., *J. Amer. Chem. Soc.* **102,** 7206 (1980). (*b*) Sato, S., and White, J. M., *Ind. Eng. Chem. Prod. Res. Dev.* **19,** 542 (1980). (*c*) Sato, S., and White, J. M., *Chem. Phys. Lett.* **70,** 131 (1980). (*d*) Sato, S., and White, J. M., *Chem. Phys. Lett.* **72,** 83 (1980). (*e*) Sato, S., and White, J. M., *J. Cataly.* **69,** 128 (1981). (*f*) Sato, S., and White, J. M., *J. Phys. Chem.* **85,** 592 (1981).
9. (*a*) Tauster, S. J., Fung, S. C., and Garten, R. L., *J. Amer. Chem. Soc.* **100,** 170 (1978). (*b*). Tauster, S. J., Fung, S. C., Baker, R. T., and Horsley, J. A., *Science* **211,** 1121 (1981).
10. (*a*) Vannice, M. A., and Garten, R. L., *J. Catal.* **56,** 236 (1979). (*b*) Vannice, M. A., and Garten, R. L., *J. Catal.* **66,** 242 (1980).
11. Tanaka, K., and White, J. M., *J. Phys. Chem.*, in press.

12. Hammaker, R. M., Francis, S. A., and Eischens, R. P., *Spectrochim. Acta* **21,** 1295 (1965).
13. Blyholder, G., *J. Phys. Chem.* **68,** 2772 (1964).
14. Hollins, P., and Pritchard, J., *ACS Symp. Ser.* **137,** 51 (1980).
15. Reinalda, D., and Ponec, V., *Surface Sci.* **91,** 113 (1979).
16. Tanaka, K., Watters, K. L., and Howe, R. F., *J. Catal.* **75,** 23 (1982).
17. Campuzano, J. C., and Greenler, R. G., *Surface Sci.* **83,** 301 (1979).
18. Bradshaw, A. M., and Hoffman, F. M., *Surface Sci.* **72,** 513 (1978).
19. Chen, B.-H., and White, J. M., *J. Phys. Chem.*, in press.
20. Collins, D. M., Lee, J. B., and Spicer, W. E., *Surface Sci.* **55,** 389 (1976).
21. Ertl, G., Neumann, M., and Streit, K. M., *Surface Sci.* **64,** 393 (1977).
22. Winicur, D. H., Hurst, J., Becker, C. A., and Wharton, L., *Surfae Sci.* **109,** 263 (1981).
23. McCabe, R. W., and Schmidt, L. D., *Surface Sci.* **65,** 189 (1977).
24. Campbell, C. T., Ertl, G., Kuipers, H., and Segner, J., *Surface Sci.* **107,** 207 (1981).
25. Collins, D. M., and Spicer, W. E., *Surface Sci.* **69,** 85 (1977).
26. McClellen, M. R., Gland, J. L., and McFeeley, F. R., *Surface Sci.* **112,** 63 (1981).
27. Bartok, M., Sarkany, J., and Sitkei, A., *J. Catal.* **72,** 236 (1981).
28. Baker, R. T., Prestridge, E. B., and Garten, R. L., *J. Catal.* **59,** 293 (1979).
29. Dubois, L., and Somorjai, G. A., *ACS Symp. Ser.* **137,** 166 (1980).
30. Campbell, C. T., Ertl, G., Kuipers, H., and Segner, J., *Surface Sci.* **107,** 220 (1981).
31. (*a*) Yates, J. T., Jr., Duncan, T. M., Worley, S. D., and Vaughan, R. W., *J. Chem. Phys.* **70,** 1219 (1979). (*b*) Yates, D. J. C., Murrell, L. L., and Prestridge, E. B., *J. Catal.* **57,** 41 (1979). (*c*) Cavanagh, R. R., and Yates, J. T., Jr., *J. Chem. Phys.* **74,** 4150 (1981).
32. Cavanagh, R. R., and Yates, J. T., Jr., *J. Catal.* **68,** 22 (1981).
33. Apple, T. M., and Dybowski, C., *J. Catal.* **71,** 316 (1981).